Description and crystal structure of liversidgeite, $Zn_6(PO_4)_4 \cdot 7H_2O$, a new mineral from Broken Hill, New South Wales, Australia

PETER ELLIOTT,[1,2,*] GERALD GIESTER,[3] EUGEN LIBOWITZKY,[3] AND UWE KOLITSCH[4]

[1]School of Earth and Environmental Sciences, The University of Adelaide, Adelaide, South Australia 5005, Australia
[2]South Australian Museum, North Terrace, Adelaide, South Australia 5000, Australia
[3]Institut für Mineralogie und Kristallographie, Geozentrum, Universität Wien, Althanstrasse 14, A-1090 Wien, Austria
[4]Mineralogisch-Petrographische Abteilung, Naturhistorisches Museum, A-1010 Wien, Austria

ABSTRACT

Liversidgeite, ideally $Zn_6(PO_4)_4 \cdot 7H_2O$, is a new mineral from Block 14 Opencut, Broken Hill, New South Wales, Australia. The mineral occurs as white, thin, bladed crystals and as hemispherical aggregates of radiating crystals in cavities in sphalerite-galena ore. Associated minerals are anglesite, pyromorphite, greenockite, sulfur, and an unknown Zn phosphate sulfate. Individual crystals are up to 0.1 mm in length and 0.05 mm across. Liversidgeite is transparent to translucent, with a vitreous luster and a white streak. It is brittle with an irregular fracture, the Mohs hardness is ~3–3.5, and the observed and calculated densities are 3.21(2) and 3.28 g/cm^3, respectively. Chemical analysis by electron microprobe gave ZnO 54.62, MnO 0.49, PbO 0.18, P_2O_5 32.62, As_2O_5 0.65, SO_3 0.35, H_2O 14.04, total 102.95 wt%, with H_2O content derived from the refined crystal structure. The empirical formula calculated on the basis of 23 O atoms is $Pb_{0.01}(Zn_{5.86}Mn_{0.06})_{\Sigma5.92}(P_{4.01}As_{0.05}S_{0.04})_{\Sigma4.10}O_{16.20} \cdot 6.8H_2O$. Liversidgeite is triclinic, space group $P\bar{1}$, with $a = 8.299(1)$, $b = 9.616(1)$, $c = 12.175(1)$ Å, $\alpha = 71.68(1)$, $\beta = 82.02(1)$, $\gamma = 80.18(1)°$, $V = 905.1(2)$ $Å^3$ (single-crystal data), and $Z = 2$. The six strongest lines in the X-ray powder diffraction pattern are [d(Å), (I), (hkl)]: 8.438 (80) (011), 3.206 (60) (01$\bar{3}$), 2.967 (75) (2$\bar{1}$2, 114), 2.956 (75) (21$\bar{2}$), 2.550 (85) (233, 2$\bar{1}$3), 2.537 (100) (22$\bar{1}$, 01$\bar{4}$, 31$\bar{1}$). The crystal structure of liversidgeite was refined to an $R1$ index of 5.95% based on 3054 observed ($F_o > 4\sigma F_o$) reflections measured with Mo$K\alpha$ X-radiation. The structure is based on two distinct, infinite zigzag chains of edge-sharing $Zn\phi_6$ (ϕ = unspecified anion) octahedra that extend in the a direction. The chains link to each other via common corners and also via corner-sharing PO_4 tetrahedra, forming sheets parallel to the (011) plane. The sheets link via $[Zn_2\phi_8]$ dimeric building units, comprising edge-sharing $Zn\phi_5$ trigonal bipyramids and $Zn\phi_4$ tetrahedra, resulting in an open framework. Large ellipsoidal channels extend along the a direction and are occupied by interstitial H_2O groups and the H atoms of the H_2O groups that coordinate to the Zn cations. An extensive network of hydrogen bonds provides additional linkage between the sheets in the structure, via the interstitial H_2O groups. The topology of the liversidgeite structure is identical to that of synthetic, monoclinic $Zn_2Co_4(PO_4)_4(H_2O)_5 \cdot 2H_2O$.

Keywords: Liversidgeite, new mineral species, zinc phosphate, crystal structure, Broken Hill, New South Wales, Australia

INTRODUCTION

The Broken Hill Pb-Zn-Ag deposit is one of the world's most famous mineral localities and is well known for providing mineral specimens of both great aesthetic and scientific value. Almost 300 mineral species are known to occur in the orebody, and Broken Hill is the type locality for 12 species (Birch 1999). Between the mid-1970s and the early 2000s, as a result of opencut mining operations to recover remnant oxidized ore from the old South Mine leases, some 75 mineral species new to Broken Hill were identified, principally from the Kintore and Block 14 Opencuts (Birch and van der Heyden 1988, 1997; Birch 1990). In 2000, a specimen of a secondary Zn phosphate mineral was collected from stockpiles of ore mined from the Block 14 Opencut. The powder X-ray diffraction pattern did not match that of any known Zn phosphate, either mineral or synthetic compound, and subsequent studies confirmed the presence of a new mineral species. Liversidgeite is named for Archibald Liversidge (1846–1927), Professor of Geology and Mineralogy, and later Professor of Mineralogy and Chemistry at the University of Sydney. The name is in recognition of his contributions to the study of the mineralogy of New South Wales, in particular that of the Broken Hill deposit, and also recognizes his contribution to science education, especially in mineralogy and chemistry. The mineral and its name have been approved by the IMA Commission on New Minerals, Nomenclature and Classification (IMA 2008-048). The type specimen of liversidgeite is lodged in the South Australian Museum collection (registration number G32512).

OCCURRENCE

The Broken Hill Pb-Zn-Ag deposit, the largest base metal orebody in the world, consists of a series of parallel, stratigraphically controlled Ag-Pb-rich and Zn-Pb-rich lenses. The sulfides and enclosing metasedimentary, pegmatitic, and metavolcanic

* E-mail: peter.elliott@adelaide.edu.au

rocks have undergone several high-grade metamorphic and deformation events (Willis et al. 1983). The orebody has a long and complex history of erosion and weathering, which has resulted in an extensive oxidized zone that reaches a depth of 100 m and is notable for the complexity of its mineralogy (e.g., Birch and van der Heyden 1997; Birch 1999). The lower portion of the oxidized zone grades into Ag-rich supergene mineralization, comprising coronadite, quartz, kaolinite, and goethite (van der Heyden and Edgecombe 1990). Between this and the sulfide zone is an irregular zone of cerussite, whose boundary with the sulfide zone is marked by a band of leached sulfides.

The specimen containing liversidgeite came from a zone of highly weathered sulfide ore in the Block 14 Opencut and comprises leached, coarse-grained sphalerite and galena with minor chalcopyrite, quartz, and fluorapatite. The new mineral has formed in cavities as a result of the release of Zn and P from the breakdown of sphalerite and fluorapatite. Associated minerals are crusts of yellow-orange greenockite, pale-yellow sulfur crystals, colorless-to-white prisms of pyromorphite, colorless crystals of anglesite and colorless, bladed crystals of an unknown Zn phosphate sulfate.

APPEARANCE, PHYSICAL AND OPTICAL PROPERTIES

Crystals of liversidgeite are thin bladed in habit (Fig. 1) and typically develop in compact radial aggregates and hemispheres. Liversidgeite is white, transparent to translucent, with a vitreous luster and a white streak. It is brittle, has an uneven fracture and a Mohs hardness of ~3–3.5. Cleavage was not observed. Individual crystals are up to 0.1 mm in length and 0.05 mm across. The density, 3.21(4) g/cm^3, was determined by the sink-float method using a Clerici-water solution, and the calculated density from the empirical formula is 3.28 g/cm^3. Optically, liversidgeite is biaxial negative and nonpleochroic. Only one, suitably large single crystal, which was used for single-crystal X-ray data collection, was available for determination of the optical properties. Crushing of a globule did not provide any suitable optically homogenous fragments. Only n_β [1.642(5)] of the flat lying crystal could be measured. The calculated n using the Gladstone-Dale relationship (Mandarino 1981) is 1.612.
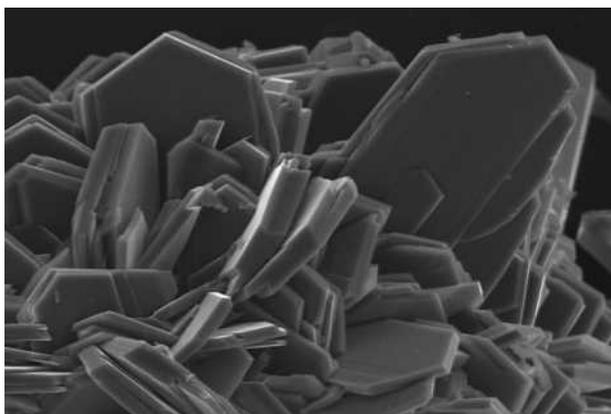
CHEMICAL ANALYSIS

A fragment of liversidgeite was embedded in epoxy, polished, and carbon coated. Wavelength-dispersive analyses were obtained using a Cameca SX51 electron microprobe operating at 15 kV and 10 nA. Data were reduced using the $\phi(\rho Z)$ method of Pouchou and Pichoir (1985). The results, as well as the standards used, are shown in Table 1. High analytical sums are due to the instability of the analyzed grain under the electron beam. Dehydration was significantly reduced by defocusing the beam to 20 µm and by micromovement of the grain during the analysis. Elements searched for but not detected were Mg, Al, Ba, Na, and F, and elements detected in amounts <0.05 wt% were Si, Cl, Ca, Fe, Cu, Cd, and K. The empirical formula calculated on the basis of 23 O atoms and water content calculated from the ideal formula from the crystal-structure solution is $Pb_{0.01}(Zn_{5.86}Mn_{0.06})_{\Sigma 5.92}(P_{4.01}As_{0.05}S_{0.04})_{\Sigma 4.10}O_{16.20} \cdot 6.8H_2O$ and the ideal formula is $Zn_6(PO_4)_4 \cdot 7H_2O$, which requires: ZnO 54.35, P_2O_5 31.60, H_2O 14.04, total 100.00 wt%.

RAMAN SPECTROSCOPY

Raman spectra of crystals of liversidgeite were recorded in the range from 4000 to 200 cm^{-1} with a Renishaw RM1000 confocal micro-Raman Imaging System using a 17 mW HeNe-laser at 632.8 nm and excitation through a Leica DMLM optical microscope [50×/0.75 N.A. objective, 180° backscatter geometry, 1200 lines/mm grating, spectral resolution (apparatus function) 4 cm^{-1}, minimum lateral resolution ~2 µm, thermo-electrically cooled CCD detector, random sample orientation]. The spectrum (Fig. 2) shows bands (strong bands italic) due to OH-stretching vibrations (broad bands 2830–2995 cm^{-1} centered on 2895, and 3095–3380 cm^{-1} centered on 3220 cm^{-1}), H-O-H bending vibration (at 1645 cm^{-1}), ν_1 and ν_3 vibrations of the PO$_4$ tetrahedra (at 1142, 1050, *1004*, *986*, and *958* cm^{-1}), and overlapping bands of the ν_4 and ν_2 vibrations of the PO$_4$ tetrahedra, vibrations of the Zn(O,H$_2$O)$_6$ octahedra and lattice modes (at 610, 584, 476, 464, 430, *244*, and 210 cm^{-1}). The O···O donor-acceptor distances of the O-H···O hydrogen bonds agree reasonably well with the positions of the OH Raman bands according to the regression curve of Libowitzky (1999).

FIGURE 1. SEM photomicrograph showing bladed crystals of liversidgeite. The field of view is 100 µm across.
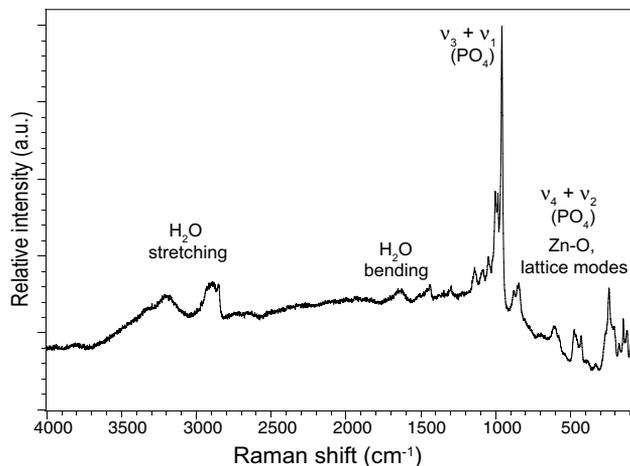
FIGURE 2. Single-crystal laser-Raman spectrum of liversidgeite.

TABLE 1. Compositional data for liversidgeite

Constituent	wt%	Range	Stand. dev.	Probe standard
ZnO	54.62	49.66–57.32	2.28	sphalerite
MnO	0.49	0.33–0.75	0.11	rhodonite
PbO	0.18	0.00–0.37	0.21	galena
P_2O_5	32.62	31.98–32.44	0.60	hydroxylapatite
As_2O_5	0.65	0.42–1.04	0.28	gallium arsenide
SO_3	0.35	0.30–0.53	0.08	chalcopyrite
H_2O*	14.04			
Total	102.95			

Note: Number of analyses = 13.
* Calculated from structure determination.

X-RAY POWDER DIFFRACTION DATA

The X-ray powder-diffraction pattern for liversidgeite (Table 2) was recorded on a 100 mm Guinier-Hägg camera using monochromatic Cr$K\alpha$ radiation (λ = 2.28970 Å). The film was scanned using a film scanner, the powder-diffraction profile was extracted and peak positions were calibrated using an internal silicon standard (NBS SRM 640a). The unit-cell parameters, a = 8.302(1), b = 9.624(1), c = 12.180(1) Å, α = 71.66(2), β = 82.01(2), γ = 80.17(3)°, V = 906.4(6) Å^3, were refined from the powder data using the Le Bail profile-fitting method (Le Bail et al. 1988), starting from the unit-cell parameters determined from single-crystal techniques. The axial ratios calculated from these cell parameters are 0.8626:1:1.2656.

SINGLE-CRYSTAL X-RAY DIFFRACTION

Single-crystal X-ray data were collected using a Bruker APEX II KappaCCD diffractometer at room temperature using Mo$K\alpha$ radiation. Unit-cell parameters, a = 8.299(1), b = 9.616(1), c = 12.175(1) Å, α = 71.68(1), β = 82.02(1), γ = 80.18(1)°, V = 905.1(2) Å^3, were obtained from least-squares refinement and are in good agreement with the parameters derived from X-ray powder data (see above). The data were reduced and corrected for Lorentz, polarization, and absorption effects. Conditions for the data collection and subsequent refinement are summarized in Table 3.

STRUCTURE SOLUTION AND REFINEMENT

Scattering curves for neutral atoms, together with anomalous dispersion corrections, were taken from *International Tables for Crystallography* (Wilson 1992). There were no systematic absences of reflections indicating that the space group lacks translational symmetry operators, and intensity statistics (mean $|E^2 - 1|$ = 0.953) clearly indicated the centrosymmetric space group $P\bar{1}$. Crystal structure solution by direct methods (SHELXS-97, Sheldrick 1997a) yielded the positions of six Zn and four P atoms. The positions of 23 O atoms were located by successive cycles of least-squares refinement and difference-Fourier synthesis (SHELXL-97, Sheldrick 1997b). At this stage of the refinement, the difference-Fourier map revealed the coordinates of 14 H atoms, belonging to the H_2O molecules, which were refined with constrained isotropic-displacement parameters and restraints on the O-H distances (~0.95 Å). Refinement of all parameters gave $R1$ = 5.95% for 3054 data with $F_o > 4\sigma(F_o)$, for a model with anisotropic-displacement parameters for all non-H atoms.

The final atomic positional parameters and displacement parameters are given in Table 4, and selected interatomic

distances and angles are given in Table 5. Table 6 contains the bond-valence analysis (Brown and Altermatt 1985; Brese and O'Keeffe 1991; Brown 1996). Table 7 presents the details of the hydrogen bonding.

CRYSTAL STRUCTURE

Cation coordination

The structure of liversidgeite contains six symmetrically independent Zn atoms, each occupied by Zn plus minor Mn. Each of the Zn1, Zn2, Zn3, and Zn4 positions is coordinated by four O^{2-} anions, and two H_2O molecules in *cis* configuration, in a distorted octahedral arrangement. Interatomic distances (Zn-O

TABLE 2. X-ray powder diffraction data for liversidgeite

I_{obs}	d_{obs}	I_{calc}	d_{calc}	hkl
30	11.507	34	11.510	001
30	9.051	52	9.045	010
80	8.438	100	8.437	011
25	6.962	12	6.954	101
30	6.522	1	6.521	111
		15	6.505	110
10	6.384	6	6.380	$10\bar{1}$
20	5.686	19	5.683	$1\bar{1}0$
		5	5.682	012
		2	4.916	102
5	4.867	11	4.863	$1\bar{1}1$
5	4.509	7	4.510	$10\bar{2}$
		6	4.319	$1\bar{1}2$
5	4.218	8	4.218	022
10	3.985	2	3.984	013
		12	3.980	211
5	3.956	4	3.954	201
		2	3.838	$02\bar{1}$
5	3.816	6	3.819	113
		2	3.815	$1\bar{1}2$
5	3.802	2	3.803	$11\bar{2}$
5	3.592	2	3.590	$12\bar{1}$
5	3.534	1	3.539	$2\bar{1}0$
5	3.481	1	3.485	$21\bar{1}$
40	3.414	27	3.419	$2\bar{1}\bar{1}$
15	3.265	9	3.260	222
60	3.206	16	3.206	$01\bar{3}$
		1	3.156	031
5	3.130	3	3.132	$02\bar{2}$
25	3.122	26	3.123	131
		2	3.096	$21\bar{3}$
5	3.005	2	3.005	$1\bar{2}\bar{3}$
		1	2.967	$12\bar{2}$
		11	2.966	$2\bar{1}\bar{2}$
75	2.967	3	2.965	114
		2	2.961	130
75	2.956	11	2.954	$21\bar{2}$
35	2.933	3	2.930	223
		3	2.929	203
5	2.920	3	2.918	$22\bar{1}$
5	2.883	2	2.878	004
20	2.846	16	2.841	124
5	2.792	8	2.791	$13\bar{1}$
15	2.726	9	2.725	$03\bar{1}$
5	2.701	1	2.708	232
20	2.678	15	2.683	$2\bar{2}\bar{2}$
		2	2.674	$20\bar{3}$
5	2.606	1	2.604	214
5	2.598	2	2.597	230
		13	2.556	233
85	2.550	6	2.554	$2\bar{1}\bar{3}$
		4	2.548	$12\bar{4}$
		8	2.547	302
		14	2.537	$22\bar{2}$
100	2.537	2	2.533	$01\bar{4}$
		9	2.532	$31\bar{1}$
15	2.483	2	2.484	034
		2	2.480	320
20	2.462	5	2.458	204
		2	2.452	$3\bar{1}1$
		1	2.432	$2\bar{2}\bar{3}$
10	2.410	9	2.409	015
5	2.395	3	2.394	$03\bar{2}$
10	2.355	3	2.356	041
		4	2.355	025
10	2.303	3	2.302	005
		3	2.281	$2\bar{3}0$
5	2.275	2	2.275	$21\bar{4}$
5	2.262	5	2.261	040
		2	2.255	$20\bar{4}$
5	2.194	2	2.200	$3\bar{2}0$
		3	2.190	$32\bar{1}$
10	2.168	1	2.168	330
		4	2.166	$2\bar{3}1$
15	2.101	2	2.104	$04\bar{1}$
		4	2.101	240
		3	2.098	$31\bar{1}$
40	2.085	4	2.085	$1\bar{2}4$
		4	2.081	$12\bar{4}$
40	2.074	3	2.072	411
5	2.046	2	2.040	244
10	2.035	1	2.036	400
		2	2.005	$13\bar{5}$
		2	1.992	026
5	1.969	4	1.970	$3\bar{2}\bar{3}$
15	1.962	2	1.963	$2\bar{1}\bar{1}$
		5	1.961	342
10	1.941	1	1.943	325
		2	1.928	343
10	1.910	5	1.909	226
		2	1.907	$3\bar{3}\bar{1}$
10	1.904	1	1.904	$14\bar{2}$
5	1.893	1	1.894	036
10	1.871	2	1.875	051
		1	1.873	$2\bar{4}0$
10	1.865	2	1.869	$3\bar{3}\bar{2}$
		4	1.869	335
		1	1.866	340
10	1.837	1	1.838	$41\bar{2}$
		1	1.828	034
5	1.813	2	1.813	251
5	1.802	1	1.800	206
5	1.775	1	1.774	$1\bar{3}4$
5	1.759	1	1.758	$34\bar{1}$
5	1.699	2	1.698	$3\bar{1}5$
5	1.688	1	1.688	353
		5	1.687	055
		2	1.684	$32\bar{4}$
5	1.673	2	1.674	$4\bar{2}2$
		2	1.667	037
		2	1.642	510

Note: Intensities estimated visually. Calculated intensities were obtained using the program LAZY PULVERIX (Yvon et al. 1977).

= 1.992 to 2.286 Å) are in agreement with those reported in the literature for Zn in sixfold coordination. The $Zn2O_6$ and $Zn3O_6$ octahedra show the more regular geometries, while the $Zn1O_6$ and $Zn4O_6$ octahedra show stronger bond-length distortions, with both representing a [5+1] coordination (Table 5). The Zn5 atom is in tetrahedral coordination, bonded to four O^{2-} anions with Zn-O distances ranging from 1.926 to 2.00 Å. The mean bond

TABLE 3. Crystal data, data collection, and refinement details

Crystal data	
Formula	$Zn_6(PO_4)_4 \cdot 7H_2O$
Space group	$P\bar{1}$
a, b, c (Å)	8.299(1), 9.616(1), 12.175(1)
α, β, γ (°)	71.68(1), 82.02(1), 80.18(1)
V (Å³), Z	905.1(2), 2
$F(000)$	842.1
μ (mm⁻¹)	7.954
Absorption correction	Multi-scan*
Crystal dimensions (mm)	$0.06 \times 0.035 \times 0.005$
Data collection	
Diffractometer	Bruker APEX II KappaCCD
Temperature (K)	293
Wavelength	$MoK\alpha, \lambda = 0.71073$ Å
θ range (°)	2.50 to 33.16
Detector distance (mm)	35
Rotation axes, width (°)	$\phi, \omega, 2$
Total no. of frames	293
Collection time per frame (s)	500
h,k,l ranges	$-12 \rightarrow 9, -14 \rightarrow 14, -18 \rightarrow 18$
Total reflections measured	13531
Data completeness (%)	94.8
Unique reflections	6566 ($R_{int} = 0.0830$)
Refinement	
Refinement on	F^2
$R1$† for $F_o > 4\sigma(F_o)$	5.95%
$wR2$‡ for all F_o^2	10.25%
Reflections used $F_o^2 > 4\sigma(F_o^2)$	3049
Number of parameters refined	355
Extinction factor	0.00017(11)
$(\Delta/\sigma)_{max}$	0.0001
$\Delta\rho_{min}, \Delta\rho_{max}$ (e/Å³)	1.24, −1.35
GooF	0.934

* Bruker (2006).
† $R1 = \Sigma||F_o| - |F_c||/\Sigma|F_o|$.
‡ $wR2 = \Sigma w(|F_o|^2 - |F_c|^2)^2/\Sigma w|F_o|^2)^{1/2}; w = 1/[\sigma^2(F_o^2) + (0.042\ P)^2 + 12.60P]. P = \{[max of (0 or F_o^2)] + 2F_c^2\}/3.$

distance of 1.964 Å compares favorably with the [4]Zn-O length (1.97 Å) calculated using the ionic radii of Shannon (1976), and with the grand mean value of 1.958 Å reported by Baur (1981). The $Zn5O_4$ tetrahedron is somewhat distorted, with two short and two long Zn-O distances. A fifth O atom is 2.82 Å from the Zn5 atom and, if included in the coordination polyhedron, would form a considerably distorted square-pyramid. The Zn6 atom is coordinated by five anions in a distorted trigonal-bipyramid with three short equatorial bonds and two elongate axial bonds (range = 1.946–2.338 Å).

The structure contains four nonequivalent P sites, each coordinated by four O atoms in a tetrahedral arrangement. The $P1O_4$ and $P4O_4$ tetrahedra show a fairly regular geometry, with P-O bond distances of 1.530, 1.531, 1.540, and 1.542 Å, and 1.521, 1.529, 1.531, and 1.538 Å, respectively. By contrast, the $P2O_4$ and $P3O_4$ tetrahedra have a less regular geometry, with the $P2O_4$ tetrahedron having two short (1.514 and 1.528 Å) and two longer (1.544 and 1.553 Å) P-O bonds, and the $P3O_4$ tetrahedron having one short (1.504 Å) and three longer (1.529, 1.530, and 1.548 Å) P-O bonds. The individual and mean P-O bond distances are within the range of commonly observed values in phosphate minerals (Baur 1981; Huminicki and Hawthorne 2002).

Structure description

The crystal structure of liversidgeite is based on infinite sheets of $Zn\phi_6$ (ϕ: O^{2-}, H_2O) octahedra and PO_4 tetrahedra (Fig. 3a), which are composed of two distinct, infinite $M\phi_4$ chains of octahedra. Pairs of edge-sharing $Zn1\phi_6$ octahedra and pairs of edge-sharing $Zn2\phi_6$ octahedra form $Zn_2\phi_{10}$ dimers, which link by edge-sharing to form zigzag $Zn\phi_4$ chains that extend in the a direction. $P1O_4$ and $P4O_4$ groups link to the vertices of the shared edge of each dimer and also link to the corresponding vertices of the neighboring dimer in the chain.

The chain links in the [01$\bar{1}$] direction, by octahedral corner-sharing, to a second symmetrically distinct, but topologically identical zigzag chain which also extends in the a direction,
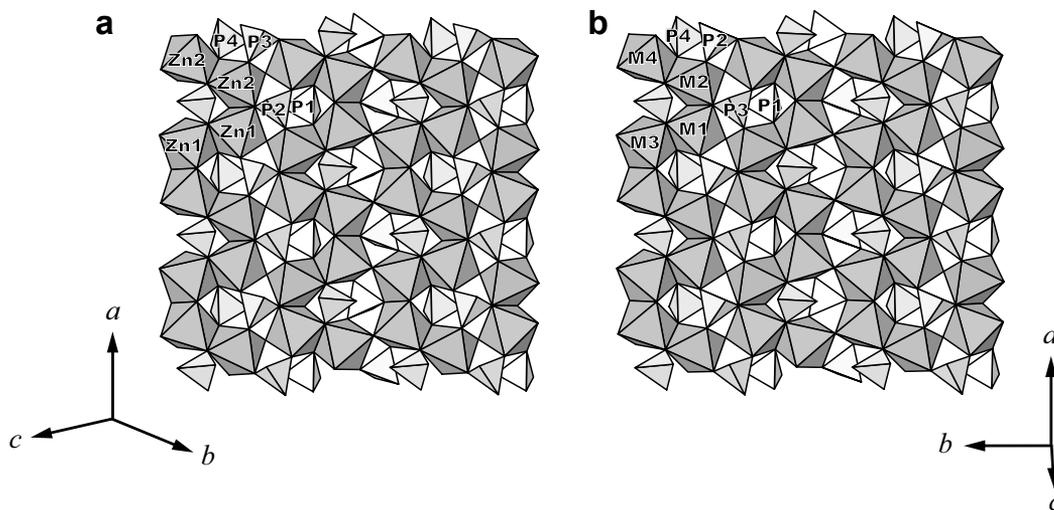
FIGURE 3. The sheets of $M\phi_6$ octahedra and PO_4 tetrahedra in the structures of (**a**) liversidgeite and (**b**) bakhchisaraitsevite, rimkorolgite, and $Zn_2Co_4(PO_4)_4(H_2O)_5 \cdot 2H_2O$ showing the difference in ordering of the M cations. All structure drawings were completed using ATOMS (Shape Software 1997).

TABLE 4. Fractional coordinates and displacement parameters (Å^2) for atoms for liversidgeite

	x	y	z	U_{eq}	U_{11}	U_{22}	U_{33}	U_{12}	U_{13}	U_{23}
Zn1	0.03028(10)	0.40116(10)	0.12441(7)	0.0119(2)	0.0105(4)	0.0141(5)	0.0102(4)	−0.0015(3)	−0.0002(3)	−0.0042(4)
Zn2	0.42699(10)	0.39460(10)	0.12045(7)	0.01177(19)	0.0121(4)	0.0102(5)	0.0114(4)	−0.0008(3)	−0.0005(3)	−0.0025(4)
Zn3	0.92638(10)	0.12078(10)	0.38843(7)	0.0117(2)	0.0105(4)	0.0136(5)	0.0095(4)	−0.0016(3)	0.0008(3)	−0.0021(4)
Zn4	0.52516(10)	0.13951(10)	0.39429(7)	0.0129(2)	0.0120(4)	0.0128(5)	0.0120(4)	0.0006(4)	−0.0008(3)	−0.0053(4)
Zn5	0.81612(10)	0.40022(10)	0.49691(7)	0.0132(2)	0.0163(4)	0.0131(5)	0.0100(4)	−0.0032(3)	0.0012(3)	−0.0037(4)
Zn6	0.64560(11)	0.33973(10)	0.74866(7)	0.0177(2)	0.0205(4)	0.0182(5)	0.0149(4)	−0.0082(4)	−0.0032(4)	0.0033(4)
P1	0.2086(2)	0.6991(2)	0.02141(14)	0.0078(4)	0.0079(8)	0.0081(10)	0.0075(8)	−0.0025(7)	−0.0008(7)	−0.0011(7)
P2	0.6794(2)	0.4369(2)	0.28472(14)	0.0077(4)	0.0084(8)	0.0063(10)	0.0080(8)	−0.0013(7)	0.0010(7)	−0.0028(7)
P3	0.1753(2)	0.3613(2)	0.36516(14)	0.0074(4)	0.0089(8)	0.0071(10)	0.0062(8)	−0.0016(7)	0.0009(7)	−0.0031(7)
P4	0.2910(2)	0.9158(2)	0.37199(14)	0.0073(4)	0.0067(8)	0.0079(10)	0.0071(8)	−0.0021(7)	0.0012(7)	−0.0026(7)
O1	0.0677(6)	0.6148(5)	0.0218(4)	0.0132(11)	0.015(3)	0.014(3)	0.009(2)	−0.001(2)	0.001(2)	−0.003(2)
O2	0.2031(5)	0.8396(5)	−0.0822(4)	0.0130(11)	0.009(2)	0.013(3)	0.014(2)	−0.002(2)	0.001(2)	0.000(2)
O3	0.3744(5)	0.6021(5)	0.0098(4)	0.0119(10)	0.011(2)	0.012(3)	0.010(2)	−0.001(2)	0.007(2)	−0.004(2)
O4	0.1947(6)	0.7373(5)	0.1365(4)	0.0138(11)	0.018(3)	0.013(3)	0.010(2)	−0.001(2)	−0.002(2)	−0.004(2)
O5	0.8043(6)	0.4742(6)	0.1804(4)	0.0162(12)	0.012(2)	0.025(3)	0.009(2)	−0.002(2)	0.005(2)	−0.004(2)
O6	0.6928(6)	0.5217(6)	0.3695(4)	0.0177(12)	0.023(3)	0.016(3)	0.014(2)	−0.003(2)	−0.004(2)	−0.004(2)
O7	0.7035(5)	0.2698(5)	0.3497(4)	0.0105(10)	0.008(2)	0.012(3)	0.012(2)	−0.002(2)	0.002(2)	−0.007(2)
O8	0.5050(5)	0.4795(5)	0.2414(4)	0.0127(11)	0.010(2)	0.015(3)	0.014(2)	−0.007(2)	0.003(2)	−0.002(2)
O9	0.3076(6)	0.2489(5)	0.4275(4)	0.0121(10)	0.014(2)	0.009(3)	0.008(2)	0.0039(19)	−0.003(2)	0.000(2)
O10	0.1726(6)	0.5127(6)	0.3821(4)	0.0176(12)	0.026(3)	0.012(3)	0.017(3)	−0.009(2)	0.001(2)	−0.004(2)
O11	0.0202(5)	0.3805(5)	0.2346(4)	0.0103(10)	0.010(2)	0.014(3)	0.007(2)	−0.0022(19)	0.0004(19)	−0.006(2)
O12	0.0069(5)	0.3072(5)	0.4133(4)	0.0102(10)	0.011(2)	0.013(3)	0.008(2)	−0.004(2)	0.0022(19)	−0.005(2)
O13	0.2963(6)	1.0072(5)	0.2447(4)	0.0128(11)	0.017(3)	0.013(3)	0.010(2)	−0.002(2)	−0.001(2)	−0.006(2)
O14	0.1269(5)	0.9595(5)	0.4349(4)	0.0119(10)	0.012(2)	0.012(3)	0.012(2)	−0.004(2)	0.001(2)	−0.003(2)
O15	0.4312(5)	0.9409(5)	0.4301(4)	0.0096(10)	0.011(2)	0.009(3)	0.009(2)	−0.0027(19)	0.0020(19)	−0.006(2)
O16	0.3041(5)	0.7509(5)	0.3821(4)	0.0113(10)	0.013(2)	0.011(3)	0.009(2)	−0.002(2)	0.003(2)	−0.006(2)
H_2O17	0.0070(6)	1.1697(6)	0.2131(4)	0.0137(11)	0.015(3)	0.015(3)	0.012(2)	−0.003(2)	−0.001(2)	−0.006(2)
H1	−0.078(6)	1.148(8)	0.190(6)	0.02(2)						
H2	0.108(6)	1.124(10)	0.202(8)	0.06(3)						
H_2O18	0.2664(6)	0.3276(6)	0.0254(4)	0.0133(11)	0.012(2)	0.015(3)	0.010(2)	−0.001(2)	−0.002(2)	−0.001(2)
H3	0.293(11)	0.232(5)	0.039(7)	0.05(3)						
H4	0.259(10)	0.380(7)	−0.050(4)	0.04(2)						
H_2O19	0.7807(6)	0.9662(6)	0.3748(4)	0.0143(11)	0.015(3)	0.010(3)	0.014(3)	0.004(2)	0.002(2)	−0.007(2)
H5	0.824(9)	0.952(8)	0.309(4)	0.03(2)						
H6	0.768(11)	0.882(7)	0.431(5)	0.05(3)						
H_2O20	0.5167(6)	0.1782(6)	0.2098(4)	0.0144(11)	0.013(3)	0.011(3)	0.017(3)	0.001(2)	0.002(2)	−0.006(2)
H7	0.444(10)	0.117(10)	0.212(9)	0.08(3)						
H8	0.613(7)	0.173(12)	0.171(9)	0.10(4)						
H_2O21	0.4575(8)	0.2074(7)	0.8254(6)	0.0389(16)	0.035(4)	0.030(4)	0.047(4)	−0.012(3)	0.019(3)	−0.009(3)
H9	0.495(17)	0.128(11)	0.886(8)	0.16(5)						
H10	0.412(18)	0.180(16)	0.771(9)	0.17(5)						
H_2O22	0.8697(8)	0.7764(7)	0.2441(6)	0.0396(16)	0.039(4)	0.033(4)	0.047(4)	−0.017(3)	0.009(4)	−0.005(3)
H11	0.827(11)	0.689(8)	0.280(9)	0.09(4)						
H12	0.977(6)	0.749(10)	0.222(8)	0.07(3)						
H_2O23	0.2714(12)	0.0512(8)	0.0136(6)	0.064(3)	0.134(8)	0.039(5)	0.033(4)	−0.018(3)	0.010(5)	−0.046(5)
H13	0.253(13)	−0.006(11)	−0.031(7)	0.09(3)						
H14	0.216(13)	0.018(12)	0.085(5)	0.10(4)						

Note: The anisotropic displacement factors (U_{ij}) are defined as $\exp[-2\pi^2\Sigma_{i=1}^3\Sigma_{j=1}^3 U_{ij}\mathbf{a}_i^* \mathbf{a}_j^* h_i h_j]$.

and comprises dimers of edge-sharing $Zn3\phi_6$ octahedra and edge-sharing $Zn4\phi_6$ octahedra. Further linkage between chains is provided by corner-sharing $P2O_4$ and $P3O_4$ groups, which link to vertices of the shared edge between each dimer and also to two vertices of $Zn\phi_6$ octahedra in adjacent dimers of the neighboring chain. The result is a complex sheet parallel to the (011) plane.

The sheets link in the [011] direction via $Zn_2\phi_8$ dimeric building units, which comprise distorted edge-sharing $Zn6\phi_5$ trigonal bipyramids and $Zn5\phi_4$ tetrahedra (Fig. 4). The resulting topology can be classified as a member of the group of phosphate minerals whose structures are based on infinite frameworks (Huminicki and Hawthorne 2002). Large ellipsoidal interstitial channels between the sheets extend along the *a* direction and are occupied by interstitial H_2O groups H_2O22 and H_2O23 and the hydrogen atoms of the H_2O17, H_2O18, H_2O20, H_2O21, and H_2O22 groups, which coordinate to the Zn^{2+} cations.

Bond-valence analysis and hydrogen bonding

There are 23 anion sites in the structure, each occupied by an O atom. The bond-valence sums for the O1, O3, O7, O8,

O10, O11, O12, O14, O15, and O16 sites are within the range of 1.97–2.12 valence units (v.u.) (Table 6), indicating that they are O^{2-} anions and it is unlikely that they accept any hydrogen bonds. The O4, O5, O6, and O9 atoms have bond-valence sums of 1.75–1.83 v.u., indicating that these are somewhat underbonded O^{2-} anions that are likely acceptors of hydrogen bonds. The O2 and O13 atoms are bonded to one P atom only and have bond valence-sums of 1.26 and 1.30 v.u., respectively, neglecting contributions of hydrogen bonds, so might be expected to be OH groups. Both anions are, however, acceptors of strong to moderate hydrogen bonds, with O···O distances of 2.550–2.809 Å. The O2 and O13 anions each receive bond-valence contributions from three H atoms bonded to three H_2O groups. These contributions increase the bond-valence sums of O2 and O13 to 1.97 and 2.00 v.u., respectively. Hence, these sites are considered to be O^{2-} anions. In addition, O2 and O13 are involved in the shortest P-O distances of their respective tetrahedra and it is highly unlikely that these O atoms are protonated, as P-OH distances are, in general, longer than P-O distances in monoprotonated phosphate groups (average P-OH = 1.581 Å; Ferraris and Ivaldi

TABLE 5. Selected interatomic distances (Å) and angles (°) for liversidgeite

Zn1-O5	1.993(5)	Zn2-O3	2.041(5)
Zn1-O11	2.035(4)	Zn2-H$_2$O20	2.084(5)
Zn1-O1	2.091(5)	Zn2-O8	2.111(4)
Zn1-O1	2.114(4)	Zn2-O3	2.120(4)
Zn1-H$_2$O17	2.176(5)	Zn2-O11	2.164(4)
Zn1-H$_2$O18	2.280(5)	Zn2-H$_2$O18	2.172(5)
<Zn-O>	2.115	<Zn-O>	2.115
Zn3-O14	2.055(4)	Zn4-O9	1.987(5)
Zn3-H$_2$O17	2.075(5)	Zn4-O7	2.009(4)
Zn3-O14	2.080(5)	Zn4-O15	2.082(5)
Zn3-H$_2$O19	2.126(5)	Zn4-O15	2.093(4)
Zn3-O12	2.135(5)	Zn4-H$_2$O20	2.167(5)
Zn3-O7	2.147(5)	Zn4-H$_2$O19	2.497(5)
<Zn-O>	2.103	<Zn-O>	2.139
Zn5-O6	1.925(4)	Zn6-O4	1.946(4)
Zn5-O10	1.925(4)	Zn6-O8	1.987(5)
Zn5-O12	1.998(4)	Zn6-O16	2.007(4)
Zn5-O16	2.000(4)	Zn6-H$_2$O21	2.110(6)
<Zn-O>	1.964	Zn6-O10	2.338(5)
		<Zn-O>	2.078
P1-O1	1.530(5)	P2-O5	1.514(5)
P1-O2	1.531(5)	P2-O6	1.528(5)
P1-O3	1.540(5)	P2-O7	1.544(5)
P1-O4	1.542(5)	P2-O8	1.553(5)
<P-O>	1.536	<P-O>	1.535
P3-O9	1.504(5)	P4-O13	1.521(5)
P3-O10	1.529(5)	P4-O14	1.529(5)
P3-O11	1.530(4)	P4-O15	1.531(5)
P3-O12	1.548(5)	P4-O16	1.538(5)
<P-O>	1.530	<P-O>	1.528
O1-P1-O2	109.5(3)	O5-P2-O6	111.1(3)
O1-P1-O3	109.8(3)	O5-P2-O7	110.9(3)
O2-P1-O3	108.6(3)	O6-P2-O7	108.6(3)
O1-P1-O4	109.8(3)	O5-P2-O8	108.4(2)
O2-P1-O4	110.7(3)	O6-P2-O8	109.3(3)
O3-P1-O4	108.4(3)	O7-P2-O8	108.5(3)
<O-P1-O>	109.5	<O-P2-O>	109.5
O9-P3-O10	111.9(3)	O13-P4-O14	109.4(3)
O9-P3-O11	110.5(3)	O13-P4-O15	110.7(3)
O10-P3-O11	107.7(3)	O14-P4-O15	109.3(2)
O9-P3-O12	108.8(3)	O13-P4-O16	109.8(3)
O10-P3-O12	108.6(3)	O14-P4-O16	107.9(3)
O11-P3-O12	109.3(2)	O15-P4-O16	109.7(3)
<O-P1-O>	109.5	<O-P1-O>	109.5

1984). The bond-valence sums for H$_2$O17, H$_2$O18, H$_2$O19, and H$_2$O20, which each coordinate to two Zn^{2+} cations, and H$_2$O21, which coordinates to the Zn6 cation, are in the range 0.33 to 0.65 v.u. and so these O atoms are H$_2$O molecules. The H$_2$O22 and H$_2$O23 groups (v.u. = 0.00) represent interstitial H$_2$O molecules not bonded to any cations, and held in the structure only by hydrogen bonds.

The structure of liversidgeite contains an extensive network of hydrogen bonds (Table 7), which can be divided into those located within the sheets of Znϕ_6 and PO$_4$ polyhedra and those between the sheets and interstitial H$_2$O groups. The hydrogen bonds can be classified as strong to weak, with O$\cdots$O distances in the range of 2.550 to 3.051 Å. Hydrogen bonds of the first type occur between H atoms of H$_2$O groups bonded to the Zn$\phi6$ octahedra and O atoms of the PO$_4$ groups. The H$_2$O17 and H$_2$O20 groups each donate two such hydrogen bonds and the H$_2$O18, and H$_2$O19 groups each one hydrogen bond. Hydrogen bonds of the second type provide additional linkage between the sheets in the structure via the interstitial H$_2$O groups. Hydrogen atoms of

TABLE 7. Details of hydrogen bonding in liversidgeite (Å, °)

D-H$\cdots$A	D-H (Å)	H$\cdots$A	D$\cdots$A	D-H$\cdots$A
H$_2$O17-H1$\cdots$O2*	0.87(4)	1.75(5)	2.550(7)	151(7)
H$_2$O17-H2$\cdots$O13	0.89(4)	1.80(5)	2.637(7)	156(9)
H$_2$O18-H3$\cdots$O23	0.87(4)	1.90(6)	2.699(9)	151(8)
H$_2$O18-H4$\cdots$O5†	0.90(4)	1.83(4)	2.698(7)	161(7)
H$_2$O19-H5$\cdots$O22	0.87(4)	2.04(6)	2.730(8)	136(6)
H$_2$O19-H6$\cdots$O9‡	0.89(4)	1.89(4)	2.740(7)	159(8)
H$_2$O20-H7$\cdots$O13§	0.91(4)	1.67(5)	2.569(7)	167(9)
H$_2$O20-H8$\cdots$O2†	0.87(4)	1.75(5)	2.623(6)	174(10)
H$_2$O21-H10$\cdots$O22‡	0.92(5)	2.33(14)	2.920(10)	122(12)
H$_2$O22-H11$\cdots$O6	0.93(5)	2.04(5)	2.956(8)	169(9)
H$_2$O22-H12$\cdots$O4‖	0.91(4)	1.96(5)	2.849(8)	164(9)
H$_2$O23-H13$\cdots$O2§	0.93(5)	1.90(6)	2.809(8)	164(9)
H$_2$O23-H14$\cdots$O13§	0.91(5)	2.11(9)	2.743(8)	126(9)
H$_2$O23-H14$\cdots$O4§	0.91(5)	2.60(10)	3.051(8)	111(8)

Note: Symmetry codes: * $-x$, $-y + 2$, $-z$; † $-x + 1$, $-y + 1$, $-z$; ‡ $-x + 1$, $-y + 1$, $-z + 1$; § x, $y - 1$, z; ‖ $x + 1$, y, z.

TABLE 6. Bond-valence analysis for liversidgeite

	Zn1	Zn2	Zn3	Zn4	Zn5	Zn6	P1	P2	P3	P4	H1	H2	H3	H4	H5	H6	H7	H8	H9	H10	H11	H12	H13	H14	Sum (excl.H)	Sum (incl.H)
O1	0.35 0.33						1.27																		1.95	1.95
O2							1.26							0.30				0.23					0.18		1.26	1.97
O3		0.40 0.33					1.23																		1.96	1.96
O4					0.52	1.23																0.18		0.11	1.75	2.03
O5	0.46							1.32							0.21										1.78	1.99
O6					0.55			1.27														0.12			1.82	1.94
O7			0.30	0.44				1.22																	1.96	1.95
O8		0.33				0.47		1.19																	1.99	1.99
O9				0.47					1.36							0.20									1.83	2.03
O10	0.41	0.29							1.27																1.99	1.99
O11				0.54	0.18				1.27																1.97	1.97
O12			0.31	0.45					1.21																1.97	1.97
O13										1.30	0.23						0.27						0.20		1.30	2.00
O14			0.39 0.36							1.27															2.02	2.02
O15				0.36						1.26															1.97	1.97
O16				0.35	0.44	0.44				1.24															2.12	2.12
H$_2$O17	0.28		0.37								0.70	0.77													0.65	2.12
H$_2$O18	0.21	0.28											0.79	0.79											0.49	2.07
H$_2$O19			0.32	0.12											0.81	0.80									0.44	2.05
H$_2$O20		0.36		0.29													0.76	0.77							0.65	2.18
H$_2$O21						0.33													1.00	0.87					0.33	2.20
H$_2$O22																			0.19		0.13	0.88	0.82		0.00	2.03
H$_2$O23									0.21														0.82	0.69	0.00	1.72
Sum	2.04	1.99	2.05	2.03	1.98	1.94	4.99	5.00	5.07	5.07	1.00	1.00	1.00	1.00	1.00	1.00	1.00	1.00	1.00	1.00	1.00	1.00	1.00	1.00		

FIGURE 4. The crystal structure of liversidgeite viewed along a direction close to [100]. $Zn\phi_6$ octahedra are pale gray; $Zn2\phi_5$ pyramids are line-shaded; $Zn3\phi_6$ tetrahedra are dark gray; PO_4 tetrahedra are cross-shaded; O atoms of water molecules are white spheres; hydrogen atoms are small gray spheres. The unit cell is outlined.

the H_2O18, H_2O19, and H_2O21 groups each donate one hydrogen bond to interstitial H_2O molecules H_2O22 and H_2O23. The H_2O22 group donates two and the H_2O23 group donates three hydrogen bonds, which are accepted by O atoms of the $Zn\phi_6$ and PO_4 polyhedra.

STRUCTURAL RELATIONS

Liversidgeite is the fifth known zinc phosphate mineral. Of these, the structures of hopeite, $Zn_3(PO_4)_2 \cdot 4H_2O$ (Hill and Jones 1976), and parahopeite, $Zn_3(PO_4)_2 \cdot 4H_2O$ (Chao 1969), are based on infinite sheets of $Zn\phi_4$ and PO_4 tetrahedra, the structure of tarbuttite, $Zn_2(PO_4)(OH)$ (Cocco et al. 1966), on chains of $Zn\phi_5$ bipyramids, and the structure of spencerite, $Zn_4(PO_4)_2(OH)_2 \cdot 3H_2O$ (Fanfani et al. 1972), on chains of $Zn\phi_4$ and PO_4 tetrahedra that link via $Zn\phi_6$ octahedra. The only other Zn mineral, which like liversidgeite contains 4-, 5-, and 6-coordinated Zn in its structure, is warikahnite, $Zn_3(AsO_4)_2 \cdot 2H_2O$ (Riffel et al. 1980).

The structure of liversidgeite is topologically identical to that of synthetic $Zn_2Co_4(PO_4)_4(H_2O)_5 \cdot 2H_2O$ (Whang et al. 1995), which is monoclinic, $P2_1/n$, and $Z = 4$. Sheets of $M\phi_6$ octahedra and PO_4 tetrahedra topologically identical to those in liversidgeite are found in the structures of bakhchisaraitsevite, $[Na_2(H_2O)_2]$ $[(Mg,Fe)_5(H_2O)_5(PO_4)_4]$ (Yakubovich et al. 2000), and rimkorolgite, $Ba[Mg_5(H_2O)_7(PO_4)_4](H_2O)$ (Krivovichev et al. 2002), which are both monoclinic, $P2_1/c$, and $Z = 4$. The relationship of the lattice parameters of bakhchisaraitsevite, rimkorolgite, and $Zn_2Co_4(PO_4)_4(H_2O)_5 \cdot 2H_2O$ to liversidgeite (li = liversidgeite) is $a \sim a_{li}$, $b \sim c_{li}$, and $c \sim 2b_{li}$. In these three structures, there is only one type of zigzag $M\phi_4$ chain, which runs along the a axis (Fig. 3b) and which is composed of edge-sharing $(Mg,Fe)\phi_6$ octahedra (bakhchisaraitsevite), $Mg\phi_6$ octahedra (rimkorolgite), or $Co\phi_6$ octahedra $[Zn_2Co_4(PO_4)_4(H_2O)_5 \cdot 2H_2O]$. Each chain links to an adjacent chain in the b direction, with adjacent chains related by a 2_1 screw axis parallel to the b axis. The sequence of cation ordering in the chains is -M1-M3-M4-M2-, while in liversidgeite

the ordering sequence in the two $M\phi_4$ chains is -Zn1-Zn1-Zn2-Zn2- and -Zn3-Zn3-Zn4-Zn4-. It is this difference in ordering of cations that results in the lowering of the symmetry of liversidgeite to triclinic, and reduction in the unit-cell volume by approximately half.

The mode of linkage between sheets differs in each of the structures. In bakhchisaraitsevite, linkage is provided by $Mg_2\phi_{10}$ dimers, which comprise two edge-sharing $Mg\phi_6$ octahedra, whereas in rimkorolgite adjacent sheets are separated by Ba^{2+} cations. The large interstitial channels in the framework of both structures extend along the b direction and are occupied by interstitial H_2O groups plus Na^+ cations (bakhchisaraitsevite) or Ba^{2+} cations (rimkorolgite). The sheets in the structure of $Zn_2Co_4(PO_4)_4(H_2O)_5 \cdot 2H_2O$ are linked by $Zn_2\phi_8$ dimeric building units, comprising edge-sharing $Zn\phi_5$ trigonal bipyramids and $Zn\phi_4$ tetrahedra.

REFERENCES CITED

Baur, W.H. (1981) Interatomic distance predictions for computer simulation of crystal structures. In M. O'Keeffe and A. Navrotsky, Eds., Structure and Bonding in Crystals II, p. 31–52. Academic Press, New York.

Birch, W.D. (1990) Minerals from the Kintore and Block 14 Opencuts, Broken Hill, N.S.W.: a review of recent discoveries, including tsumebite, kipushite, and otavite. Australian Mineralogist, 5, 125–141.

——— (1999) The minerals. In W.D. Birch, Ed., Minerals of Broken Hill, p. 88–256. Broken Hill Council, New South Wales.

Birch, W.D. and van der Heyden, A. (1988) Minerals of the Kintore Opencut, Broken Hill, New South Wales. Mineralogical Record, 19, 425–436.

——— (1997) Minerals from the Kintore and Block 14 Open cuts, Broken Hill, New South Wales. Australian Journal of Mineralogy, 3, 23–71.

Brese, N.E. and O'Keeffe, M. (1991) Bond-valence parameters for solids. Acta Crystallographica, B47, 192–197.

Brown, I.D. (1996) VALENCE: a program for calculating bond-valences. Journal of Applied Crystallography, 29, 479–480.

Brown, I.D. and Altermatt, D. (1985) Bond-valence parameters obtained from a systematic analysis of the inorganic crystal structure database. Acta Crystallographica, B41, 244–247.

Bruker (2006) SADABS. Bruker AXS, Inc., Madison, Wisconsin.

Chao, G.Y. (1969) Refinement of the crystal structure of parahopeite. Zeitschrift für Kristallographie, 130, 261–266.

Cocco, G., Fanfani, L., and Zanazzi, P.F. (1966) The crystal structure of tarbuttite, $Zn_2(OH)PO_4$. Zeitschrift für Kristallographie, 23, 321–329.

Fanfani, L., Nunzi, A., and Zanazzi, P.F. (1972) Structure and twinning in spencerite. Mineralogical Magazine, 38, 687–692.

Ferraris, G. and Ivaldi, G. (1984) X–OH and O–H···O bond lengths in protonated oxoanions. Acta Crystallographica, B40, 1–6.

Hill, R.J. and Jones, J.B. (1976) The crystal structure of hopeite. American Mineralogist, 61, 987–995.

Huminicki, D.M.C. and Hawthorne, F.C. (2002) The crystal chemistry of the phosphate minerals. In M.J. Kohn, J. Rakovan, and J.M. Hughes, Eds., Phosphates: Geochemical, Geobiological, and Materials Importance, 48, p. 123–253. Reviews in Mineralogy and Geochemistry, Mineralogical Society of America, Chantilly, Virginia.

Krivovichev, S.V., Britvin, S.N., Burns, P.C., and Yakovenchuk, V.N. (2002) Crystal structure of rimkorolgite, $Ba[Mg_5(H_2O)_7(PO_4)_4](H_2O)$, and its comparison with bakhchisaraitsevite. European Journal of Mineralogy, 14, 397–402.

Le Bail, A., Duroy, H., and Fourquet, J.L. (1988) Ab-initio structure determination of $LiSbWO_6$ by X-ray powder diffraction. Materials Research Bulletin, 23, 447–452.

Libowitzky, E. (1999) Correlation of O-H stretching frequencies and O-H···O hydrogen bond lengths in minerals. Monatshefte für Chemie, 130, 1047–1059.

Mandarino, J.A. (1981) The Gladstone-Dale relationship: Part IV: The compatibility concept and its application. Canadian Mineralogist, 19, 441–450.

Pouchou, J.L. and Pichoir, F. (1985) "PAP" $\phi(\rho Z)$ procedure for improved quantitative microanalysis. In J.T. Armstrong, Ed., Microbeam Analysis, 104–106.

San Francisco Press, California.

Riffel, H., Keller, P., and Hess, H. (1980) Die Kristallstruktur von Warikahnit, $Zn_3[(H_2O)_2](AsO_4)_2$. Tschermaks Mineralogische und Petrographische Mitteilungen, 27, 187–199.

Shannon, R.D. (1976) Revised effective ionic radii and systematic studies of interatomic distances in halides and chalcogenides. Acta Crystallographica, A32, 751–767.

Shape Software (1997) ATOMS for Windows and Macintosh V 4.0. Kingsport, Tennessee.

Sheldrick, G.M. (1997a) SHELXS-97, a program for the solution of crystal structures. University of Göttingen, Germany.

——— (1997b) SHELXL-97, a program for crystal structure refinement. University of Göttingen, Germany.

van der Heyden, A. and Edgecombe, D.R. (1990) Silver-lead-zinc deposit at South Mine, Broken Hill. In F.E. Hughes, Ed., Geology of the Mineral Deposits of Australia and Papua New Guinea, p. 1073–1077. The Australasian Institute of Mining and Metallurgy, Parkville, Victoria.

Whang, D.M., Hur, N.H., and Kim, K. (1995) A novel microporous mixed-transition-metal phosphate: Hydrothermal synthesis, characterization, and structure of $Zn_2Co_4(PO_4)_4(H_2O)_5 \cdot 2H_2O$. Inorganic Chemistry, 34, 3363–3366.

Willis, I.L., Brown, R.E., Stroud, W.J., and Stevens, B.P.J. (1983) The Early Proterozoic Willyama Supergroup: Stratigraphic sub-division and interpretation of high to low grade metamorphic rocks in the Broken Hill Block, N.S.W. Journal of the Geological Society of Australia, 30, 195–224.

Wilson, A.I.C. (1992) International Tables for Crystallography, vol. C, 883p. Kluwer Academic, Dordrecht.

Yakubovich, O.V., Massa, W., Liferovich, R.P., and Pakhomovsky, Y.A. (2000) The crystal structure of bakhchisaraitsevite, $[Na_2(H_2O)_2]\{(Mg,Fe)_5(H_2O)_5(PO_4)_4\}$, a new mineral species of hydrothermal origin from the Kovdor phoscorite-carbonatite complex, Russia. Canadian Mineralogist, 38, 831–838.

Yvon, K., Jeitschko, W., and Parthé, E. (1977) LAZY PULVERIX, a computer program, for calculating X-ray and neutron diffraction powder patterns. Journal of Applied Crystallography, 10, 73–74.